Adverse effects of fluoroquinolone antibiotics on onset and exacerbation of aortic aneurysm and dissection

フルオロキノロン系抗菌薬による大動脈瘤・解離の発症増悪の有害作用

Koshun Inada

Content

Abbreviations 2
General introduction 3
References 5

Chapter1
Section1: Moxifloxacin induces aortic aneurysm and dissection by increasing osteopontin in mice

1. Introduction 8
2. Materials and Methods 10
3. Results 13
4. Discussion 19

Chapter1
Section2: Moxifloxacin increases osteopontin expression through phosphorylation of ERK1/2 and JNK in macrophages

1. Introduction 22
2. Materials and Methods 23
3. Results 25
4. Discussion 30
References 32

Chapter2: Fluoroquinolone antibiotics exacervate aortic anurysm and dissection by decreasing the expression of marker of the vascular smooth muscle cells contractile phenotype

1. Introduction 37
2. Materials and Methods 39
3. Results 42
4. Discussion 50
References 52
General discussion 54
Published and submitted papers 55
Acknowledgments 56

Abbreviations

AAA; abdominal aortic aneurysm

AAD; aortic aneurysm and dissection

CPFX; ciprofloxacin

ERK1/2; extracellular signal-regulated kinase 1/2

JNK; c-Jun N-terminal kinase

LVFX; levofloxacin

MFLX; moxifloxacin

MMP; matrix metalloproteinase

OPN; osteopontin

RASMCs; rat aortic smooth muscle cells

SM22α; smooth muscle 22α

SMMHC; smooth muscle myosin heavy chain

VSMCs; vascular smooth muscle cells

α-SMA; α-smooth muscle actin

General introduction

The fluoroquinolone antibiotics moxifloxacin (MFLX), ciprofloxacin (CPFX), and levofloxacin (LVFX), are among the most commonly prescribed antibiotics. They act by inhibiting microbial DNA gyrase and topoisomerase IV, has a wide spectrum, and excellent pharmacokinetics, including good tissue distribution. However, the use of fluoroquinolones is associated with a substantial increase in the risk of cardiovascular mortality; among them, MFLX was found to have the highest probability of such events, with a 2- to 3-fold increase in risk [1]. In addition, further clinical research and a meta-analysis highlighted that the use of fluoroquinolones increases the risk of aortic aneurysm and dissection (AAD) [2, 3]. Furthermore, the Food and Drug Administration and European Medicine Agency identified that MFLX, CPFX, and LVFX are strongly associated with aortic aneurysm and dissection (AAD) [4]. On January 10, 2019, the Ministry of Health, Labor, and Welfare instructed pharmaceutical companies to revise their package inserts to add the following to the serious side effects for all fluoroquinolone antibiotics: "May cause aortic aneurysm and aortic dissection."

AAD cause extensive dilation of major blood vessel, ultimately leading to aortic rupture. Risk factors for AAD include smoking, old age, male sex, and hypertension [5-9]. Abdominal aortic aneurysm (AAA) is generally characterized by focal dilation of > 50% above the normal average aortic diameter. Pathological features of AAA include extracellular matrix degradation and loss of vascular smooth muscle cells (VSMCs), associated with inflammatory cell infiltration in the media and adventitia. In most cases, AAA is asymptomatic, with an 85 to 90% mortality after rupture [10]. However, there is currently no drug therapy recommended for the stabilization of AAA [11].

Despite the frequent use of fluoroquinolone antibiotics which have been shown to be effective for a wide range of infectious diseases, the increased risk of AAD is a serious problem. However, at present, almost no basic research on the onset mechanism of AAD exists, and a considerable lack of clarity remains. The present thesis aimed to elucidate the pathogenesis of AAD induced by fluoroquinolone antibiotics to establish preventive measures and avoid AAD as an adverse effect of fluoroquinolone antibiotics. In particular, in section 1 of the first chapter, we investigated the impact of MFLX on the occurrence of AAD in a moderate-severity mouse model. In section 2 of the first chapter, we investigated the effect of MFLX on the expression of OPN protein in RAW264.7 cells (a murine macrophage cell line). In the second chapter, we focused on VSMC phenotype switching and loss involved in the onset and exacerbation of AAA and a comparative study with phenotype switching and loss in RASMCs among three drugs, MFLX, CPFX and LVFX.

References

[1] E. Gorelik, R. Masarwa, A. Perlman, V. Rotshild, M. Abbasi, M. Muszkat, I. Matok, Fluoroquinolones and cardiovascular risk: A systematic review, meta-analysis and network meta-analysis, Drug Saf 42 (2019) 529-538.

[2] C.C. Lee, M.T. Lee, Y.S. Chen, S.H. Lee, Y.S. Chen, S.C. Chen, S.C. Chang, Risk of aortic dissection and aortic aneurysm in patients taking oral fluoroquinolone, JAMA Intern Med 175 (2015) 1839-1847.

[3] S. Singh, A. Nautiyal, Aortic dissection and aortic aneurysms associated with fluoroquinolones: A systematic review and meta-analysis, Am J Med 130 (2017) 1449-1457.e1449.

[4] A.C. Bennett, C.L. Bennett, B.J. Witherspoon, K.B. Knopf, An evaluation of reports of ciprofloxacin, levofloxacin, and moxifloxacin-association neuropsychiatric toxicities, long-term disability, and aortic aneurysms/dissections disseminated by the Food and Drug Administration and the European Medicines Agency, Expert Opin Drug Saf 18 (2019) 1055-1063.

[5] E. Altobelli, L. Rapacchietta, V.F. Profeta, R. Fagnano, Risk factors for abdominal aortic aneurysm in population-based studies: A systematic review and meta-analysis, Int J Environ Res Public Health 15 (2018).

[6] K.C. Kent, R.M. Zwolak, N.N. Egorova, T.S. Riles, A. Manganaro, A.J. Moskowitz, A.C. Gelijns, G. Greco, Analysis of risk factors for abdominal aortic aneurysm in a cohort of more than 3 million individuals, J Vasc Surg 52 (2010) 539-548.

[7] S. Aggarwal, A. Qamar, V. Sharma, A. Sharma, Abdominal aortic aneurysm: A comprehensive review, Exp Clin Cardiol 16 (2011) 11-15.

[8] P.E. Norman, J.A. Curci, Understanding the effects of tobacco smoke on the pathogenesis of aortic aneurysm, Arterioscler Thromb Vasc Biol 33 (2013) 1473-1477.

[9] M. Landenhed, G. Engström, A. Gottsäter, M.P. Caulfield, B. Hedblad, C. Newton-Cheh, O. Melander, J.G. Smith, Risk profiles for aortic dissection and ruptured or surgically treated aneurysms: a prospective cohort study, J Am Heart Assoc 4 (2015) e001513.

[10] K.C. Kent, Clinical practice. Abdominal aortic aneurysms, N Engl J Med 371 (2014) 2101-2108. 10.1056/NEJMcp1401430.

[11] V.B. Kokje, J.F. Hamming, J.H. Lindeman, Editor's Choice - Pharmaceutical management of small abdominal aortic aneurysms: A systematic review of the clinical evidence, Eur J Vasc Endovasc Surg 50 (2015) 702-713. 10.1016/j.ejvs.2015.08.010.

Chapter 1

Section 1

Moxifloxacin induces aortic aneurysm and dissection by increasing osteopontin in mice

1. Introduction

Fluoroquinolones are among the most frequently prescribed antibiotics. The fluoroquinolone moxifloxacin (MFLX) is widely used in urinary tract, gastrointestinal, and respiratory infections. It acts by inhibiting microbial DNA gyrase and topoisomerase IV, has a wide spectrum, and excellent pharmacokinetics, including good tissue distribution. However, side effects include gastrointestinal and central nervous system symptoms, tendon rupture, retinal detachment, renal and liver damage. Furthermore, the use of fluoroquinolones is associated with a substantial increase in the risk of cardiovascular mortality; among them, MFLX was found to have the highest probability of such events, with a 2- to 3-fold increase in risk [1]. In addition, further clinical research and a meta-analysis highlighted that the use of fluoroquinolones increases the risk of aortic aneurysm and dissection (AAD) [2,3].

Risk factors for AAD include smoking, old age, male sex, hypertension [4-8]. AAD have histological features such as weakening of aortic vessel walls through aortic medial degeneration due to vascular smooth muscle cell (VSMCs) loss and injury, and elastic fiber destruction and depletion by matrix metalloproteinase (MMP)-2 and -9. Thus, MMP-2 and -9 are critical to the occurrence of AAD [9]. Smooth muscle protein 22α (SM22α) is a marker of the VSMC contractile phenotype [10]. The levels of expression of SM22α mRNA and protein are lower in the aortic wall of abdominal aortic aneurysm (AAA) model animals than in controls [11].

Osteopontin (OPN) is a marker for the VSMCs synthetic phenotype [10], plays important roles in cardiovascular diseases and inflammation [12] and upregulates MMP-2 expression in aortic tissues isolated from rats with induced AAA [13].

Furthermore, the expression levels of OPN in the plasma and aortic wall are higher in patients with AAA and aortic dissection (AD) than in healthy controls [14]. Serum OPN positively correlates with MMP-2 levels in patients with AD [15]. Therefore, OPN is considered to be critical to the occurrence of AAD.

The mechanism underlying fluoroquinolone-induced AAD remains unclear. In the present study, we examined the involvement of OPN in the pathogenesis of MFLX-induced AAD using a moderate-severity AAD model in mice.

2. Materials and Methods

2.1. Animals

Four-week-old male C57BL/6J mice were purchased from Charles River Laboratories Japan (Yokohama, Japan) and housed under standard conditions of humidity (40–60%), temperature (20–26℃), under a regular dark-light cycle (12-h light/dark cycle, lights on at 7 a.m.), and with free access to food and water. All experimental protocols were approved by the Laboratory Animal Care and Use Committee of Fukuoka University. All experimental animals were handled in accordance with the Law for the Protection and Management of Animal (Law No. 105, 1973) and Standards Relating to the Care and Management of Laboratory Animals and Relief of Pain (No. 88, 2006) of the Japanese Government. C57BL/6J mice (4 weeks old) were fed a high-fat diet (1.25% cholesterol, 15% cacao butter, and 0.5% sodium cholate; F2HFD1; Oriental Yeast Co., Tokyo, Japan). Four weeks later (8 weeks old), mice were subcutaneously implanted with an osmotic minipump (Alzet model 2004; Durect, CA, USA), and infused with angiotensin II (Sigma-Aldrich, MO, USA) for four consecutive weeks [16]. MFLX (Cayman Chemical Company, MI, USA) or distilled water was orally administered to mice for three weeks. At 12 weeks, mice were euthanized and perfused with ice-cold phosphate-buffered saline (PBS). The aorta was excised and analyzed using immunohistochemical staining and western blotting.

2.2. Hematoxylin eosin (H&E) and Elastica-van Gieson (EVG) staining

The abdominal aortic segments were frozen in optimal cutting temperature (OCT) compound (Sakura FineTech, Tokyo, Japan). The tissues were cut into 7 μm slices. For H&E staining, tissues were stained in Mayer's hematoxylin solution for 1 minute (min),

washed in running tap water for 10 min and with distilled water, and then stained in eosin solution for 3 min. For EVG staining, tissues were inserted in 1% HCl and 70% ethanol solutions for 1 min, resorcin-fuchsin solution modified by Maeda for 60 min, washed under running tap water for 10 min, treated with Weigert's iron hematoxylin staining for 5 min, washed under running tap water for 10 min, and inserted in van Gieson solution for 10 min. Then, stained tissues were dehydrated with ethanol and xylene and mounted on cover glass using Mount-Quick (Daido Sangyo Co., Ltd. Saitama, Japan). Abdominal aortic tissues were observed under a BZ-X710 microscope (Keyence Corporation, Osaka, Japan).

2.3. Immunohistochemical staining

The abdominal aortic segments were frozen in OCT Compound (Sakura FineTech) and cut into 7 μm slices. The tissues were stained using the VECTASTAIN ABC Kit (Vector Laboratories, CA, USA). The primary antibodies used were rabbit anti-SM22α (1:200 dilution; Proteintech, IL, USA), rabbit anti-OPN (1:200 dilution; Abcam, Cambridge, UK), and rabbit anti-MMP-2 (1:100 dilution; Santa Cruz Biotechnology, TX, USA). A peroxidase substrate solution was prepared using a peroxidase staining DAB kit (Nacalai Tesque, Kyoto, Japan). The tissues were then dehydrated with ethanol and xylene and mounted on cover glass using Mount-Quick (Daido Sangyo Co., Ltd.). Abdominal aortic tissues were observed under a BZ-X710 microscope (Keyence Corporation).

2.4. Western blot

Proteins were isolated from aortic tissues using a lysis buffer (50 mM HEPES, 50 mM NaCl, 5 mM EDTA, 1% Triton X-100, 1 mM Na_3VO_4, 50 mM NaF, 10 mM NaPP, and 1

mM PMSF) containing 1% phosphatase and 1% protease inhibitor cocktail (Nacalai Tesque). Equal amounts (20 μg) of total protein were subjected to sodium dodecyl sulfate (SDS) polyacrylamide gel electrophoresis (10.5%) and transferred to polyvinylidene difluoride membranes (Millipore, MA, USA), followed by incubation with Blocking One (Nacalai Tesque) for 60 min at 20–28 °C.

The primary antibodies used were rabbit anti-SM22α (1:1000 dilution; Proteintech), mouse anti-OPN (1:100 dilution; Santa Cruz Biotechnology), rabbit anti-MMP-2 (1:1000 dilution; Santa Cruz Biotechnology), and rabbit anti-ß-actin (1:1000 dilution; Bioss Antibodies, MA, USA).

The membranes were incubated with primary antibodies overnight at 4 °C and then incubated with secondary horseradish peroxidase-conjugated antibodies (1:10000 dilution; Bio-Rad Laboratories, CA, USA) for 60 min at 20–28 °C. Membranes were developed using ImmunoStar® LD (Fujifilm Wako Pure Chemical Corporation, Osaka, Japan). Images were digitally captured using the FluorChem SP imaging system (Alpha Innotech, CA, USA). Signal intensities were quantified using ß-actin, and band intensities were quantified using ImageJ software.

2.5. Statistical analyses

Statistical analyses were performed using GraphPad Prism 9 software (GraphPad, CA, USA). Data are presented as mean ± standard error of the mean (SEM). The statistical significance of comparisons among the three groups was determined using one-way analysis of variance (ANOVA) with Tukey's multiple comparisons post hoc test. Statistical significance was set at $p < 0.05$.

3. Results

3.1. Impact of MFLX on the occurrence of AAA in mice with moderate-severity AAD

We investigated the impact of MFLX on the occurrence of AAD in mice with moderate AAD severity. In mice with moderate-severity AAD, MFLX (30 and 100 mg kg^{-1} day^{-1}) induced AAD in the abdominal aorta (Fig. 1A).

Next, histological changes in the aortic tissues of mice with moderate-severity AAD were characterized by H&E and EVG staining. MFLX (30 and 100 mg kg^{-1} day^{-1}) treatment for 21 days, but not vehicle administration, induced aortic dilatation and destruction (Fig. 1B).

Moreover, elastic fiber fragmentation and loss of smooth muscle cells were observed in the aortic media in MFLX (30 and 100 mg kg^{-1} day^{-1})-treated moderate AAD model mice when compared with control mice (Fig. 2A).

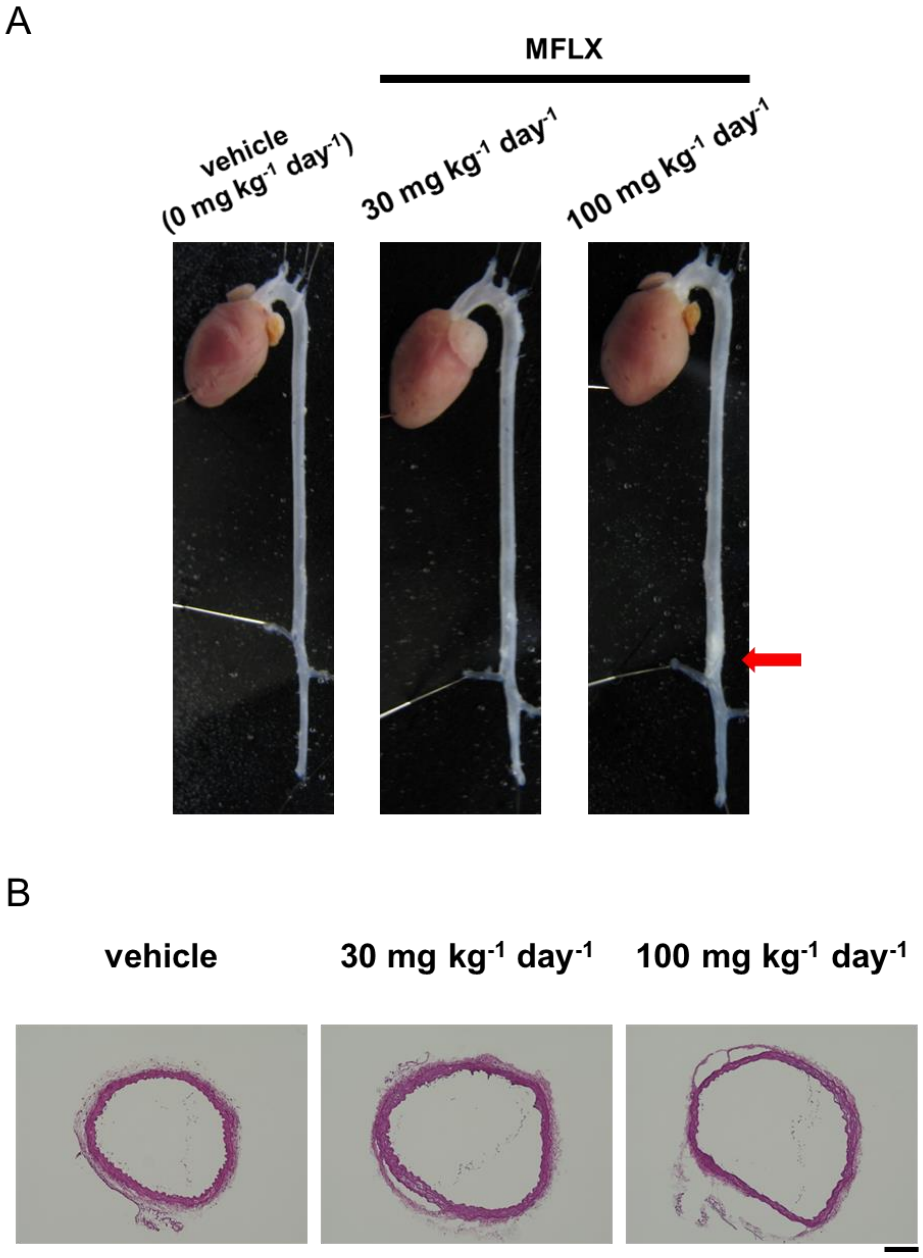

Fig. 1 Impact of MFLX on AAD occurrence in mice with moderate severity AAD
C57BL/6J mice (4 weeks old) fed a high-fat diet for 8 weeks were infused with angiotensin II (1000 ng kg-1 min-1) the first 4 weeks, and then administered vehicle or MFLX (30 and 100 mg kg-1 day-1) for 3 weeks. Representative images of the aorta showing different features following administration of vehicle or MFLX (30 and 100 mg kg-1 day-1). The red arrow indicates AAD features (A). Hematoxylin and eosin (H&E) stained-tissues shows aortic dilatation and destruction in treated-mice vs. control (B). Scale bar: 100 μm.

3.2. Effects of MFLX on expression of AAD-related proteins assessed by immunohistochemical analysis

Next, we examined the effect of MFLX on the expression levels of AAD-related proteins - SM22α (a VSMCs marker), OPN, and MMP-2, in the aortic media of experimental mice by immunohistochemical analysis. MFLX decreased the expression of SM22α in the aortic tissue media compared to vehicle (Fig. 2B). In addition, MFLX treatment increased the expression of OPN and MMP-2 in aortic tissues compared to vehicle-treatment (Fig. 2C and D).

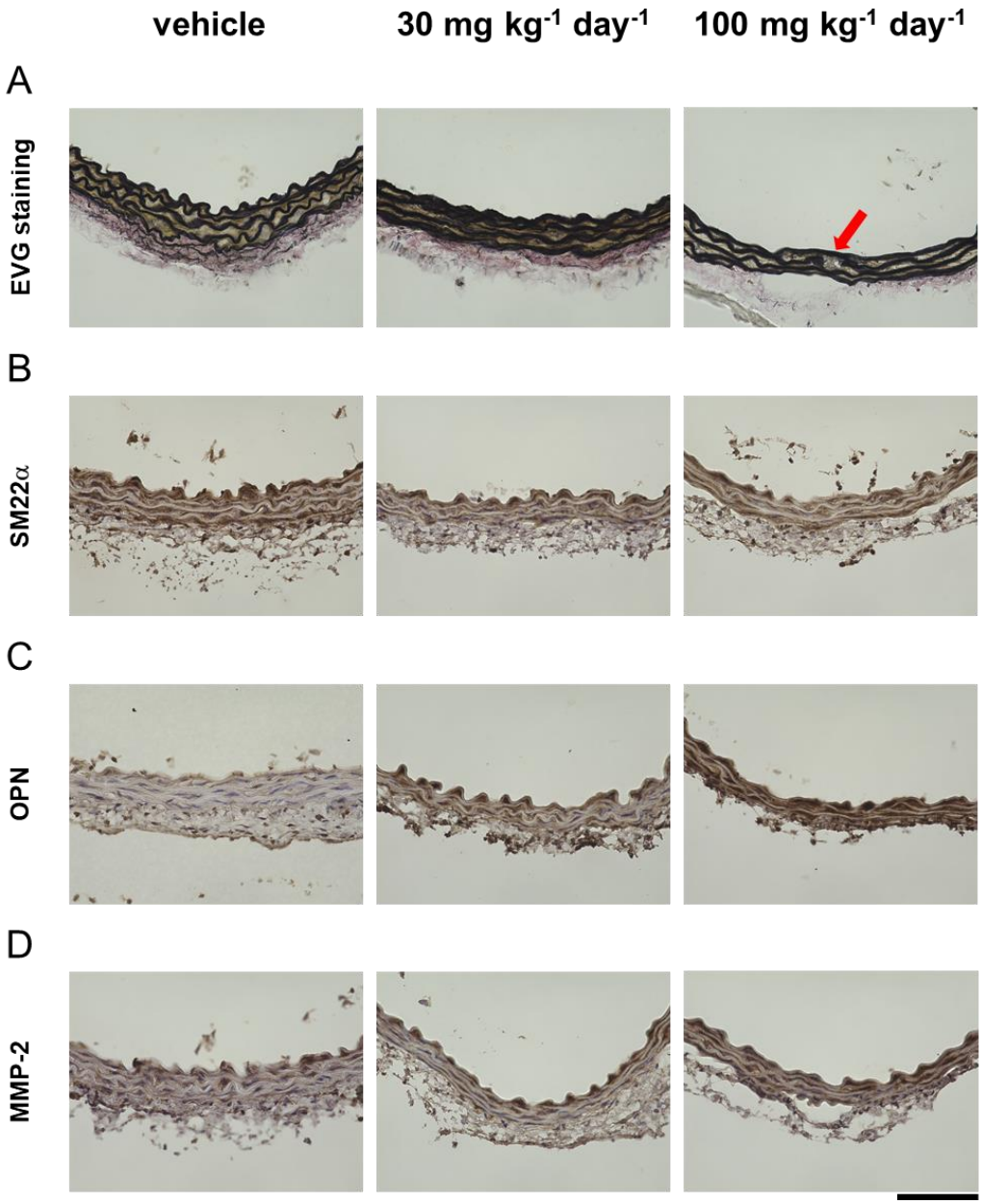

Fig. 2 Effects of MFLX on the expression of SM22α, OPN, and MMP-2 in aortic vessel wall assessed by immunohistochemical analysis

C57BL/6J mice (4 weeks old) were fed a high-fat diet for 8 weeks, infused with angiotensin II in the first 4 weeks, and then administered vehicle or MFLX (30 and 100 mg kg-1 day-1) for 3 weeks. Representative images of Elastica-van Gieson (EVG) staining showing differences in fragmentation of elastic fibers between treated- and control groups. The red arrow indicates fragmentation of elastic fibers in the aortic vessel wall (A). Immunohistochemical staining shows the expression of SM22α (B), OPN (C), and MMP-2 (D). Scale bar: 100 μm.

3.3. Effects of MFLX on the expression of AAD-related proteins assessed by western blot analysis

Immunoblot analysis showed that compared to vehicle administration, treatment with MFLX for 21 days dose-dependently decreased the expression of SM22α in aortic vessel walls in mice with moderate-severity AAD (Fig. 3A). The protein levels of SM22α expression were significantly lower in the high-dose MFLX group (100 mg kg^{-1} day^{-1}) than those in the low-dose group (30 mg kg^{-1} day^{-1}) (60%, $p < 0.01$). In addition, MFLX increased the expression of OPN and MMP-2 proteins in the aortic vessel walls in mice with moderate-severity AAD when compared to control. The level of OPN protein expression in aortic vessel walls was significantly higher in MFLX groups (30 and 100 mg kg^{-1} day^{-1}) than in control mice (400% and 420%, respectively, each $p < 0.05$) (Fig. 3B). Furthermore, the level of MMP-2 protein expression in aortic vessel walls was significantly higher in MFLX groups (30 and 100 mg kg^{-1} day^{-1}) than in control mice (135%, $p < 0.05$ and 143%, $p < 0.01$, respectively) (Fig. 3C).

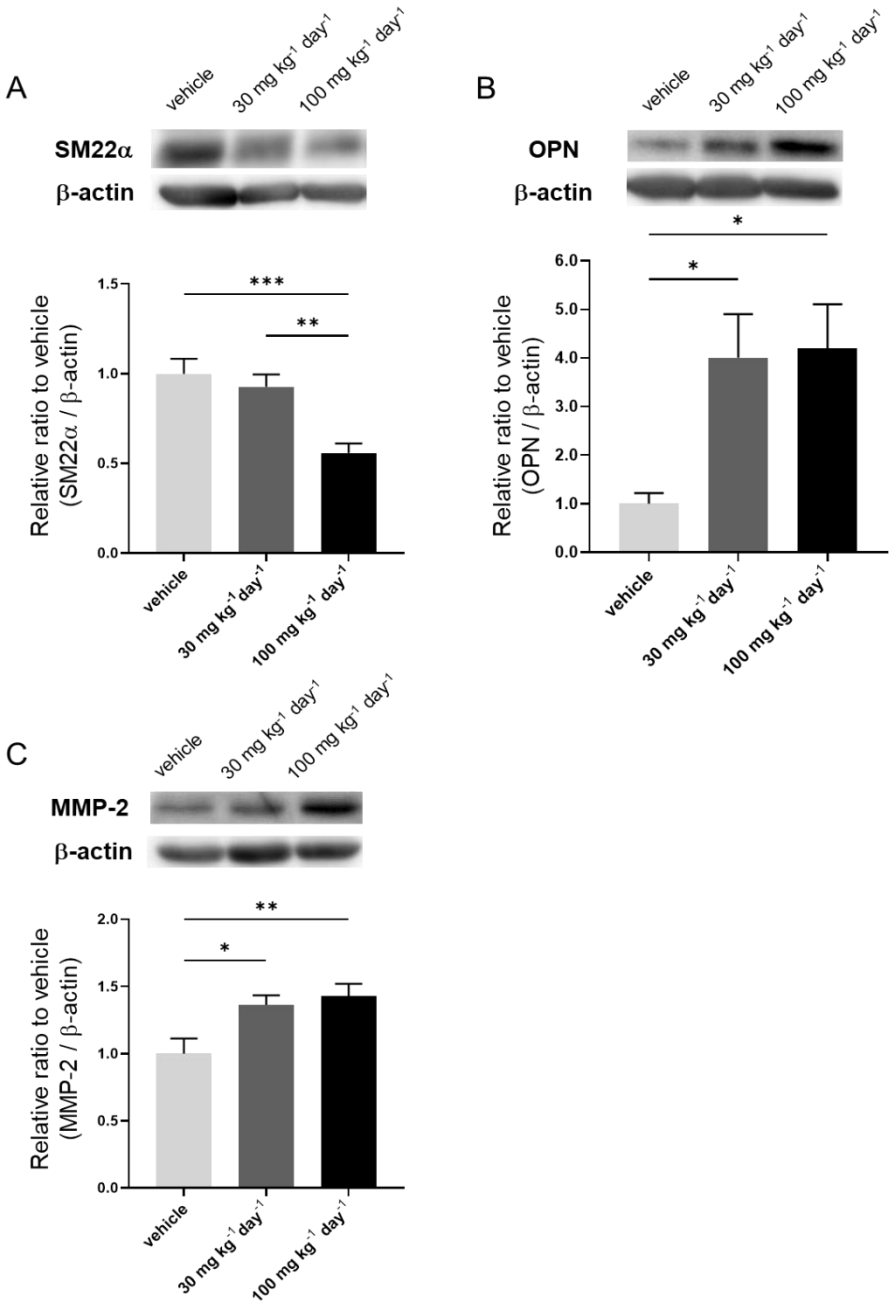

Fig. 3 Effects of MFLX on the levels of protein expressions for SM22α, OPN, and MMP-2 in aorta assessed by immunoblot analysis

C57BL/6J mice (4 weeks old) were fed a high-fat diet for 8 weeks and infused with angiotensin II for the first 4 weeks and then administered with vehicle or MFLX (30 and 100 mg kg-1 day-1) for 3 weeks. Immunoblot analysis shows the levels of protein expression for SM22α (A), OPN (B), and MMP-2 (C). Bars represent mean ± SD; *P<0.05, **P<0.01, ***P<0.001.

4. Discussion

The use of fluoroquinolones increases the risk of AAD [2,3]. In addition, the fluoroquinolone ciprofloxacin (CPFX) was shown to increase aortic dissection and rupture in mice with moderate-severity AAD [16]. However, little is known about the mechanism of fluoroquinolone-induced AAD. Therefore, in the present study, we examined the effect of MFLX, a fluoroquinolone, on AAD occurrence in mice with moderate-severity AAD.

Mice with moderate-severity AAD were treated with MFLX (30 and 100 mg kg^{-1} day^{-1}) by oral administration. MFLX (100 mg kg^{-1} day^{-1}) induced AAD in a moderate-severity AAD mouse model [Fig. 1A]. Moreover, we observed pathological features of AAD, including aortic dilatation, destruction, elastic fiber fragmentation, and loss of smooth muscle cells in aortic tissues. Therefore, MFLX may increase the risk for AAD by weakening the aortic wall.

VSMCs play an important role in maintaining the vascular structure and regulating vessel wall contraction or relaxation. Phenotype switching in VSMCs from contractile to synthetic induces aortic aneurysm [17] and AD [18]. MFLX decreased the expression of SM22α, one of the markers of the VSMC contractile phenotype, in AAD tissues of mice with moderate-severity AAD when compared to control mice [Fig. 2B and 3A]. In addition, MFLX increased the expression of OPN, a marker of the VSMCs synthetic phenotype, in the AAD tissues of mice with moderate-severity AAD when compared to control mice [Fig. 2C and 3 B]. These results demonstrate that MFLX promotes the contractile-to-synthetic conversion of VSMCs and thus, may induce AAD formation.

OPN expression levels are higher in patients with small AAA (diameter 30–50 mm)

than in patients with occlusive disease (diameter < 30 mm) or large AAA (diameter > 50 mm) [19]. In the present study, MFLX significantly increased OPN expression in aortic tissues in mice with AAD, indicating that MFLX may initiate AAD occurrence and aggravate it at an early stage.

MFLX significantly increased the expression of MMP-2 in aortic tissues of mice with moderate-severity AAD when compared to control mice [Fig. 2D and 3C]. However, there was no significant difference in the levels of MMP-9 expression in the aortic tissues of the vehicle- and MFLX-treated groups (data not shown). In patients with AAA, OPN induced MMP activation in the abdominal aorta [20] and increased MMP-2 and -9 expression in the smooth muscle cells of the aortic media and in the inflammatory cells located in the aortic media and adventitia, respectively [21]. Therefore, MFLX may induce MMP-2 expression by increasing the levels of OPN in the aortic media but not in the aortic adventitia.

MFLX may induce the development of AAA and weaken the aortic media by increasing the expression of OPN and MMP-2 and decreasing the expression of SM22α protein in aortic tissue. Our findings support the hypothesis that the use of MFLX increases the risk of AAD. Therefore, MFLX should be used with caution in patients with cardiovascular diseases who are at a high risk of AAD.

Section 2

Moxifloxacin increases osteopontin expression through phosphorylation of ERK1/2 and JNK in macrophages

1. Introduction

Macrophages have pathogenic and protective functions in the pathophysiology of AAA by contributing to ECM remodeling, inflammation, and oxidative stress [22]. Furthermore, macrophages lead to the destruction and separation of aortic vessel wall in both humans and mice through elastic fiber degradation [23] and vascular smooth muscle cells apoptosis [24]. Thus, macrophages are involved in the onset and exacerbation of AAA.

In the first section, we demonstrated that MFLX might induce the onset of AAA and weaken the aortic media by increasing the expression of OPN protein in aortic tissue. Therefore, we examined the effect of MFLX on the expression of OPN protein in macrophages.

2. Materials and Methods

2.1. Cell culture

RAW 264.7 cells of the murine macrophage line were purchased from Riken (Saitama, Japan). These cells were seeded in 60-mm dishes at 8×10^5 cells/dish and cultured in RPMI 1640 medium containing 10% fetal bovine serum (BIO-WEST, UT, USA) and 100 U mL^{-1} penicillin/streptomycin (Nacalai Tespue, Kyoto, Japan) in a in a humidified atmosphere of 5% CO_2/95% air at 37 ºC. Cells were serum-starved for 3 h and then treated with MFLX.

2.2. Western blot analysis

Proteins were isolated from RAW 264.7 cells using lysis buffer (50 mM HEPES, 50 mM NaCl, 5 mM EDTA, 1% Triton X-100, 1 mM Na_3VO_4, 50 mM NaF, 10 mM NAPP and 1 mM PMSF) containing 1% phosphatase and 2% protease inhibitor cocktail (Nacalai Tesque). Equal amounts of total protein (30 μg/30 μL) were subjected to sodium dodecyl sulfate (SDS) polyacrylamide gel electrophoresis (10.5%) and transferred to polyvinylidene difluoride membranes (Millipore), followed by incubation with Blocking One (Nacalai Tesque) for 60 min at 20–28 °C.

The primary antibodies used were mouse anti-OPN (1:100 dilution; Santa Cruz Biotechnology), anti-phospho-extracellular signal-regulated kinase 1/2 (ERK1/2) (1:1000 dilution, Cell Signaling Technology), anti-ERK1/2 (Thr202/Tyr204) (1:1000 dilution, Cell Signaling Technology), anti-phospho stress-activated protein kinase (SAPK)/c-Jun N-terminal kinase (JNK) (Thr183/Tyr185) (1:1000 dilution, Cell Signaling Technology), anti-SAPK/JNK (1:1000 dilution, Cell Signaling Technology), and mouse

anti-glyceraldehyde 3-phosphate dehydrogenase (GAPDH) (1:2000 dilution; Millipore). The membranes were incubated with primary antibodies overnight at 4 °C, and then incubated with secondary horseradish peroxidase-conjugated antibodies (1:10000 dilution; Bio-Rad Laboratories, CA, USA) for 60 min at 20–28 °C. Membranes were developed using an ImmunoStar® LD (Fujifilm Wako Pure Chemical Corporation, Osaka, Japan). Band images were visualized using a FluorChem SP imaging system (Alpha Innotech, CA, USA). Band intensities were quantified using the ImageJ software.

2.3. Statistical analyses

Statistical analyses were performed using GraphPad Prism 9 software (GraphPad, CA, USA). Data are presented as the mean ± standard error of the mean (SEM). The statistical significance of comparisons in each graph was determined using one-way analysis of variance (ANOVA) with Tukey's multiple comparisons post hoc test. Statistical significance was set at $p < 0.05$.

3. Results

3.1. Effects of MFLX on the expression of OPN proteins in RAW264.7 cells

Treatment with MFLX (300 μM) for 24 h dramatically increased the expression of OPN protein in RAW264.7 cells (Fig. 4A).

In addition, treatment with MFLX (300 μM) time-dependently increased the expression of OPN protein in RAW264.7 cells; the highest increase was observed at 24 h (Fig. 4B).

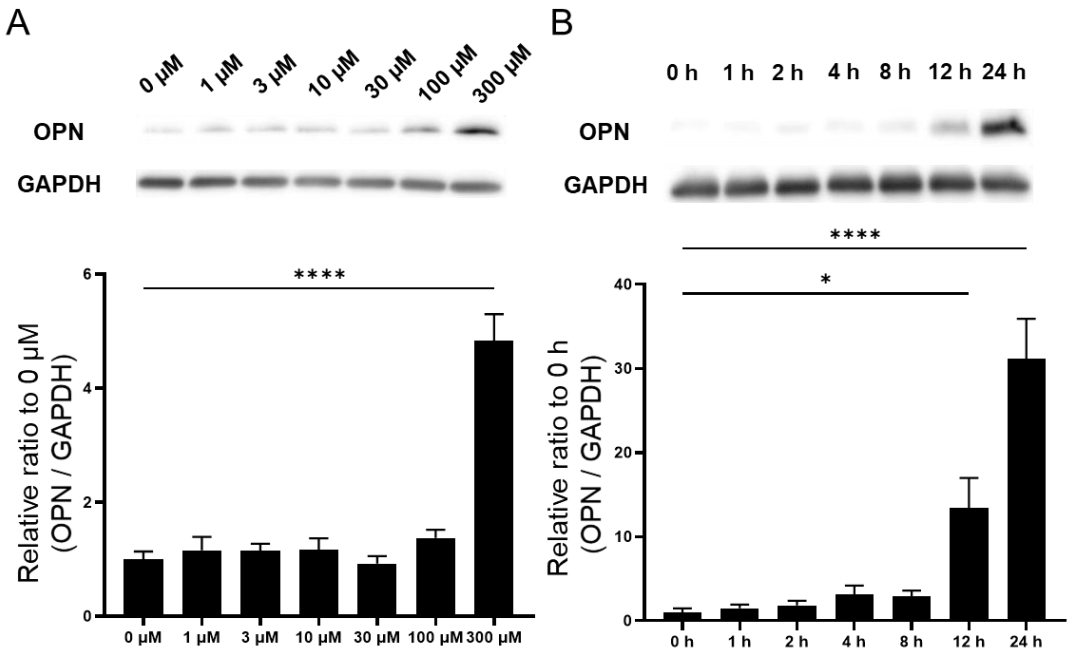

Fig. 4 Effect of MFLX on protein expression levels of OPN in RAW264.7 cells

(A) Representative immunoblots showing protein levels of OPN (upper panels). Quantitative analyses of band intensities showing expression of OPN protein (bottom panel). Protein expression levels of OPN were the highest at 300 μM MFLX. (n = 5). Bars represent the mean ± SEM; ****P < 0.0001.

(B) Representative immunoblots showing protein levels of OPN (upper panels). Quantitative analyses of band intensities showing expression of OPN protein (bottom panel). Protein expression levels of OPN were time-dependently increased from 0 to 24 h. Cells were treated with 300 μM MFLX. (n = 3).

Bars represent the mean ± SEM; *P < 0.05, ****P < 0.0001.

3.2. MFLX-induced expression of OPN protein through phosphorylation of ERK1/2 and JNK in RAW264.7 cells

To determine the activation of intracellular signaling pathways in MFLX-treated macrophages, we assessed phosphorylation of ERK1/2 and JNK pathways. MFLX induced phosphorylation of ERK1/2 and JNK compared with the baseline at 0 h (ERK1/2 and JNK: 5.2-fold increase at 8 h and 2.6-fold increase at 1 h after MFLX treatment, respectively) (Fig. 5). ERK1/2 and JNK inhibitors significantly decreased the expression of OPN protein induced by MFLX (67%, $p < 0.01$ and 33%, $p < 0.001$, respectively) (Fig. 6).

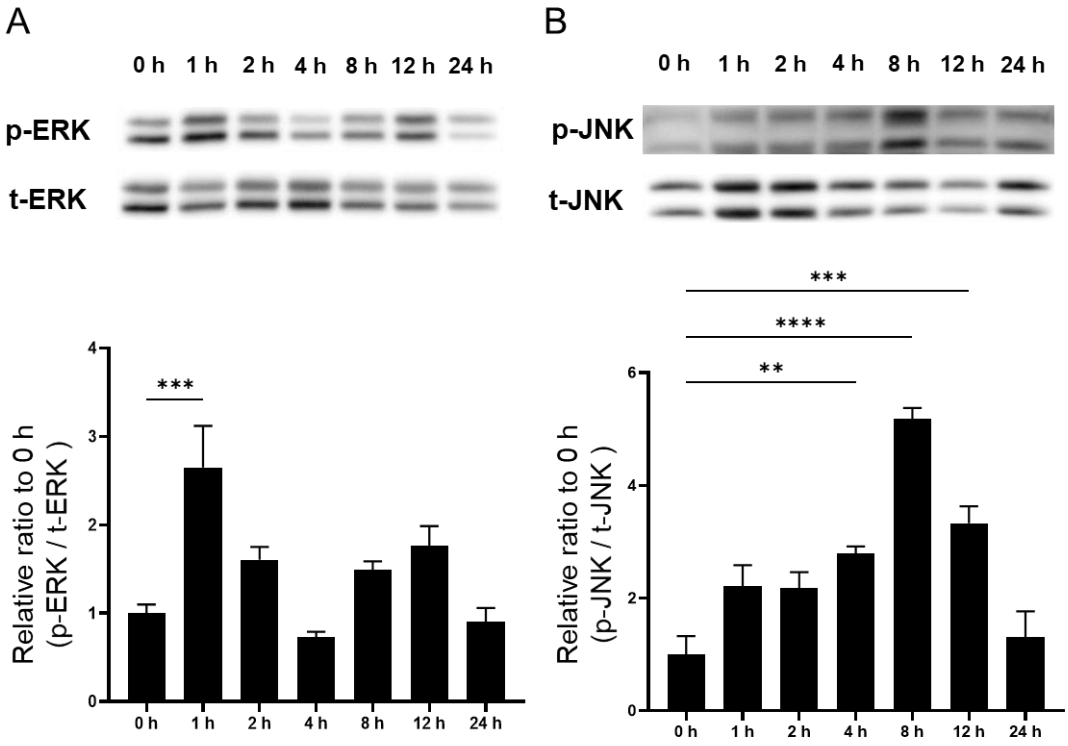

Fig. 5 MFLX-phosphorylated ERK1/2 and JNK in RAW264.7 cells

(A) Representative immunoblots (upper panels) showing protein expression of total and phosphorylated ERK1/2. Quantitative analyses of band intensities showing expression of total and phosphorylated to total proteins in untreated control cells at 0 h. Cells were treated with 300 μM MFLX for the indicated times (1, 2, 4, 8, 12, and 24 h). Bars represent the mean ± SEM (n = 4). ***P < 0.001.

(B) Representative immunoblots (upper panels) showing protein expression of total and phosphorylated JNK. Quantitative analyses of band intensities showing expression of total and phosphorylated proteins to total proteins in untreated control cells at 0 h. Cells were treated with 300 μM MFLX for the indicated times (1, 2, 4, 8, 12, and 24 h). Bars represent the mean ± SEM (n = 4). **P < 0.01, ***P < 0.001, ****P < 0.0001.

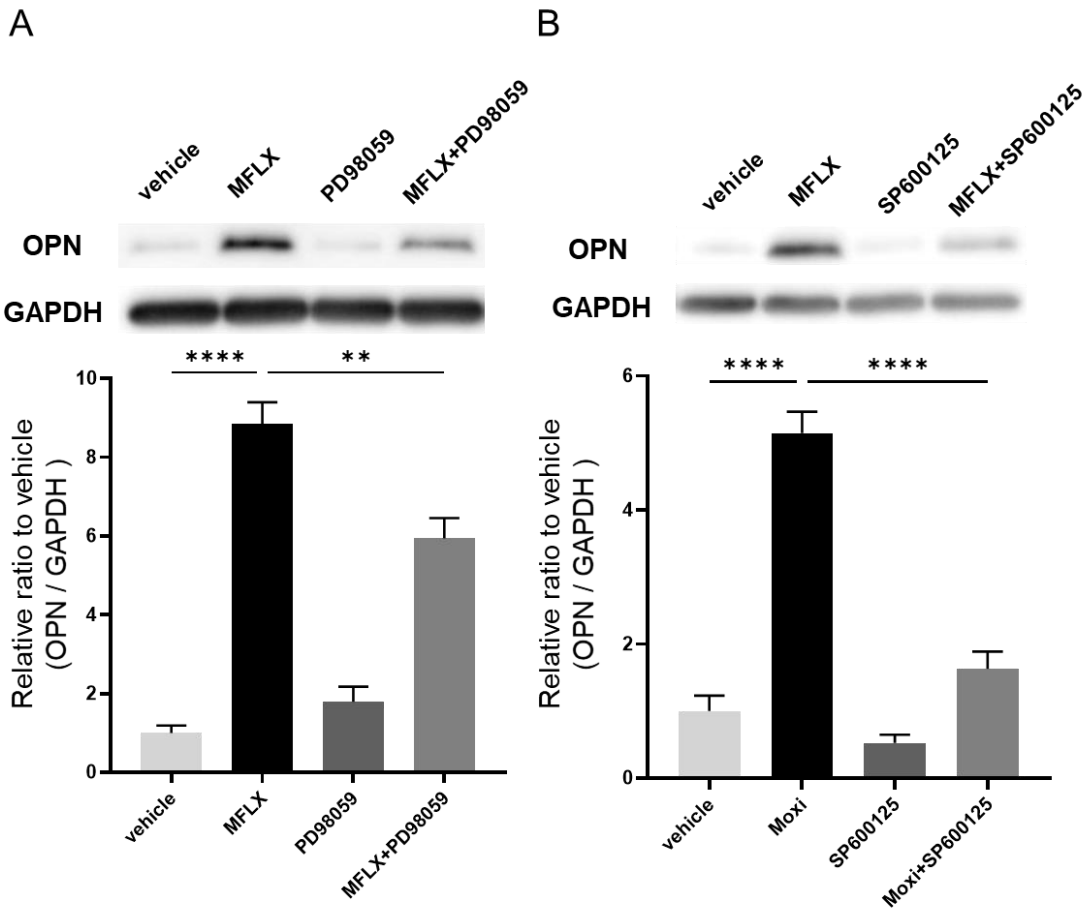

Fig. 6 Effect of ERK1/2 inhibitor (PD98059) and JNK inhibitor (SP600125) on MFLX-induced expression of OPN protein in RAW264.7 cells

Representative immunoblots showing protein levels of OPN (upper panels). Quantitative analyses of band intensities showing expression of OPN protein (bottom panel). Cells were treated with vehicle or MFLX (300 μM) for 24 h in the absence or presence of the ERK1/2 inhibitor (PD98059) (A) or the JNK inhibitor (SP600125) (B). PD98059 and SP600125 were added to cells for 30 min before treatment with vehicle or MFLX. Bars represent the mean ± SEM (n = 4). **P < 0.01, ****P < 0.0001.

4. Discussion

In this section, we provide evidence from *in vitro* experiments that MFLX increases expression of OPN protein in RAW264.7 cells (Fig. 4). Phosphorylation of ERK1/2 and JNK has an important role in the regulation of OPN gene expression [25]. Therefore, we examined activation of ERK1/2 and JNK signaling. MFLX induced phosphorylation of ERK1/2 and JNK in RAW264.7 cells (Fig. 5). However, MFLX maximally activated the ERK1/2 and JNK signaling pathways at 1 and 8 h, respectively. However, trovafloxacin has been shown to phosphorylate JNK at both 1 and 2 h in RAW264.7 cells [26]. Phosphorylation of ERK and JNK was consistent with our results. The expression of OPN was significantly decreased by an ERK1/2 inhibitor, PD98059 (20 μM), and a JNK inhibitor, SP600125 (20 μM). Therefore, ERK1/2 and JNK signaling pathways are highly likely to be responsible for MFLX-induced increase the expression of OPN in RAW264.7 cells (Fig. 6). Therefore, MFLX may induce onset and exacerbation of AAA through increased expression of OPN protein through phosphorylation of ERK1/2 and JNK in RAW264.7 cells.

Fluoroquinolone antibiotics produce and accumulate ROS in cells such as macrophages [27, 28]. In addition, ROS produces inflammatory cytokines through multiple signaling pathways such as the MAPK signaling pathway. Therefore, MFLX may increase the expression of OPN protein in macrophages through ROS accumulation. In future, the effects of MFLX on ROS production and the relationship between ROS and multiple signaling pathways should be examined to elucidate the mechanism in more detail.

Currently, most of studies have been focusing OPN, and knowledge about the role of intracellular OPN in macrophages is limited. Therefore, our understanding of

intracellular OPN in macrophages is limited. Nevertheless, it has been reported that intracellular OPN in neutrophils promoted cell migration [29]. Therefore, MFLX might contribute to the progress of inflammation through OPN-induced migrated inflammatory cells.

References

[1] C.C. Lee, M.T. Lee, Y.S. Chen, S.H. Lee, Y.S. Chen, S.C. Chen, S.C. Chang, Risk of aortic dissection and aortic aneurysm in patients taking oral fluoroquinolone, JAMA Intern Med 175 (2015) 1839-1847.

[2] S. Singh, A. Nautiyal, Aortic dissection and aortic aneurysms associated with fluoroquinolones: A systematic review and meta-analysis, Am J Med 130 (2017) 1449-1457.e1449.

[3] E. Altobelli, L. Rapacchietta, V.F. Profeta, R. Fagnano, Risk factors for abdominal aortic aneurysm in population-based studies: A systematic review and meta-analysis, Int J Environ Res Public Health 15 (2018).

[4] E. Gorelik, R. Masarwa, A. Perlman, V. Rotshild, M. Abbasi, M. Muszkat, I. Matok, Fluoroquinolones and cardiovascular risk: A systematic review, meta-analysis and network meta-analysis, Drug Saf 42 (2019) 529-538.

[5] K.C. Kent, R.M. Zwolak, N.N. Egorova, T.S. Riles, A. Manganaro, A.J. Moskowitz, A.C. Gelijns, G. Greco, Analysis of risk factors for abdominal aortic aneurysm in a cohort of more than 3 million individuals, J Vasc Surg 52 (2010) 539-548.

[6] S. Aggarwal, A. Qamar, V. Sharma, A. Sharma, Abdominal aortic aneurysm: A comprehensive review, Exp Clin Cardiol 16 (2011) 11-15.

[7] P.E. Norman, J.A. Curci, Understanding the effects of tobacco smoke on the pathogenesis of aortic aneurysm, Arterioscler Thromb Vasc Biol 33 (2013) 1473-1477.

[8] M. Landenhed, G. Engström, A. Gottsäter, M.P. Caulfield, B. Hedblad, C. Newton-Cheh, O. Melander, J.G. Smith, Risk profiles for aortic dissection and ruptured or surgically treated aneurysms: A prospective cohort study, J Am Heart Assoc 4 (2015)

e001513.

[9] E.M. Maguire, S.W.A. Pearce, R. Xiao, A.Y. Oo, Q. Xiao, Matrix metalloproteinase in abdominal aortic aneurysm and aortic dissection, Pharmaceuticals (Basel) 12 (2019).

[10] S. Allahverdian, C. Chaabane, K. Boukais, G.A. Francis, M.L. Bochaton-Piallat, Smooth muscle cell fate and plasticity in atherosclerosis, Cardiovasc Res 114 (2018) 540-550.

[11] G. Ailawadi, C.W. Moehle, H. Pei, S.P. Walton, Z. Yang, I.L. Kron, C.L. Lau, G.K. Owens, Smooth muscle phenotypic modulation is an early event in aortic aneurysms, J Thorac Cardiovasc Surg 138 (2009) 1392-1399.

[12] M.A. Icer, M. Gezmen-Karadag, The multiple functions and mechanisms of osteopontin, Clin Biochem 59 (2018) 17-24.

[13] J. Li, X. Bao, Y. Li, Y. Wang, Z. Zhao, X. Jin, Study of the functional mechanisms of osteopontin and chemokine-like factor 1 in the development and progression of abdominal aortic aneurysms in rats, Exp Ther Med 12 (2016) 4007-4011.

[14] S.K. Wang, L.A. Green, A.R. Gutwein, A.K. Gupta, C.M. Babbey, R.L. Motaganahalli, A. Fajardo, M.P. Murphy, Osteopontin may be a driver of abdominal aortic aneurysm formation, J Vasc Surg 68 (2018) 22s-29s.

[15] F. Fan, Q. Zhou, Z. Xu, D. Wang, Osteopontin in the pathogenesis of aortic dissection by the enhancement of MMP expressions, Int Heart J 60 (2019) 429-435.

[16] S.A. LeMaire, L. Zhang, W. Luo, P. Ren, A.R. Azares, Y. Wang, C. Zhang, J.S. Coselli, Y.H. Shen, Effect of ciprofloxacin on susceptibility to aortic dissection and rupture in mice, JAMA Surg 153 (2018) e181804.

[17] N. Mao, T. Gu, E. Shi, G. Zhang, L. Yu, C. Wang, Phenotypic switching of vascular smooth muscle cells in animal model of rat thoracic aortic aneurysm, Interact

Cardiovasc Thorac Surg 21 (2015) 62-70.

[18] Y. Shao, G. Li, S. Huang, Z. Li, B. Qiao, D. Chen, Y. Li, H. Liu, J. Du, P. Li, Effects of extracellular matrix softening on vascular smooth muscle cell dysfunction, Cardiovasc Toxicol 20 (2020) 548-556.

[19] J. Golledge, J. Muller, N. Shephard, P. Clancy, L. Smallwood, C. Moran, A.E. Dear, L.J. Palmer, P.E. Norman, Association between osteopontin and human abdominal aortic aneurysm, Arterioscler Thromb Vasc Biol 27 (2007) 655-660.

[20] C. Suehiro, J. Suzuki, M. Hamaguchi, K. Takahashi, T. Nagao, T. Sakaue, T. Uetani, J. Aono, S. Ikeda, T. Okura, H. Okamura, O. Yamaguchi, Deletion of interleukin-18 attenuates abdominal aortic aneurysm formation, Atherosclerosis 289 (2019) 14-20.

[21] V. Lesauskaite, M.C. Epistolato, M. Castagnini, S. Urbonavicius, P. Tanganelli, Expression of matrix metalloproteinases, their tissue inhibitors, and osteopontin in the wall of thoracic and abdominal aortas with dilatative pathology, Hum Pathol 37 (2006) 1076-1084.

[22] J. Raffort, F. Lareyre, M. Clément, R. Hassen-Khodja, G. Chinetti, Z. Mallat, Monocytes and macrophages in abdominal aortic aneurysm, Nat Rev Cardiol 14 (2017) 457-471.

[23] P. Ren, M. Hughes, S. Krishnamoorthy, S. Zou, L. Zhang, D. Wu, C. Zhang, J.A. Curci, J.S. Coselli, D.M. Milewicz, S.A. LeMaire, Y.H. Shen, Critical Role of ADAMTS-4 in the Development of Sporadic Aortic Aneurysm and Dissection in Mice, Sci Rep 7 (2017) 12351.

[24] X. Wang, H. Zhang, L. Cao, Y. He, A. Ma, W. Guo, The Role of Macrophages in Aortic Dissection, Front Physiol 11 (2020) 54.

[25] Z. Xie, M. Singh, K. Singh, ERK1/2 and JNKs, but not p38 kinase, are involved in

reactive oxygen species-mediated induction of osteopontin gene expression by angiotensin II and interleukin-1beta in adult rat cardiac fibroblasts, J Cell Physiol 198 (2004) 399-407.

[26] K.L. Poulsen, R.P. Albee, P.E. Ganey, R.A. Roth, Trovafloxacin potentiation of lipopolysaccharide-induced tumor necrosis factor release from RAW 264.7 cells requires extracellular signal-regulated kinase and c-Jun N-Terminal Kinase, J Pharmacol Exp Ther 349 (2014) 185-191.

[27] X. Wang, X. Zhao, M. Malik, K. Drlica, Contribution of reactive oxygen species to pathways of quinolone-mediated bacterial cell death, J Antimicrob Chemother 65 (2010) 520-524.

[28] R. El Bekay, M. Alvarez, M. Carballo, J. Martín-Nieto, J. Monteseirín, E. Pintado, F.J. Bedoya, F. Sobrino, Activation of phagocytic cell NADPH oxidase by norfloxacin: a potential mechanism to explain its bactericidal action, J Leukoc Biol 71 (2002) 255-261.

[29] N.A. Atai, M. Bansal, C. Lo, J. Bosman, W. Tigchelaar, K.S. Bosch, A. Jonker, P.C. De Witt Hamer, D. Troost, C.A. McCulloch, V. Everts, C.J. Van Noorden, J. Sodek, Osteopontin is up-regulated and associated with neutrophil and macrophage infiltration in glioblastoma, Immunology 132 (2011) 39-48.

Chapter 2

Fluoroquinolone antibiotics exacerbate aortic aneurysm and dissection by decreasing the expression of the vascular smooth muscle cell contractile phenotype marker

1. Introduction

Moxifloxacin (MFLX), ciprofloxacin (CPFX), and levofloxacin (LVFX) are among the most commonly prescribed fluoroquinolone antibiotics. The Food and Drug Administration and European Medicine Agency identified that MFLX, CPFX, and LVFX and are strongly associated with aortic aneurysm and dissection (AAD) [1]. Fluoroquinolone antibiotics have a wide antibacterial spectrum, and are frequently used for many infectious diseases such as urinary and respiratory infections. Furthermore, systematic reviews and meta-analyses showed that the use of fluoroquinolone antibiotics increased the risk of AAD [2, 3].

Abdominal aortic aneurysm (AAA) is generally characterized by focal dilation of > 50% above the normal average aortic diameter. The development and exacerbation of AAA involve vascular smooth muscle cell (VSMC) phenotype switching and loss, inflammation, and oxidative stress. Smoking and old age are important risk factor for the development of AAA [4, 5]. In most cases, AAA is asymptomatic, with 85 to 90% mortality after rupture [6]. However, there is currently no drug therapy recommended for the stabilization of AAA [7].

Blood vessels are composed of three layers: the intima, media, and adventitia. The media coexists with smooth muscle cells (SMCs) and the extracellular matrix. VSMCs in the blood vessel media are of the mature contractile phenotype that regulates the diameter of the blood vessel by contraction and relaxation. The transition toward the synthetic phenotype is generally characterized by the loss of proteins associated with the contractile phenotype [8]. Markers of the VSMC contractile phenotype include smooth muscle 22α (SM22α), α-smooth muscle actin (α-SMA), smooth muscle myosin

heavy chains (SMMHCs), and heavy-caldesmon (h-caldesmon) [9].

In this chapter, we focused on VSMC phenotype switching and loss involved in the onset and exacerbation of AAA, and compared the expression of VSMC contractile phenotype markers in rat aortic smooth muscle cells (RASMCs) among three drugs, MFLX, CPFX, and LVFX.

2. Materials and Methods

2.1. Rat aortic smooth muscle cell (RASMCs) culture

Male 6-8-week-old (200–250 g) Sprague–Dawley (SD) rats were purchased from Kyudo Co., Ltd (Saga, Japan). Thoracic aorta of the rats was excised after and abdominal and thoracic incision and blood evacuation. The aortas were transferred to 100-mm dishes containing D-MEM medium supplemented with 10% fetal bovine serum (BIO-WEST, UT, USA) and 100 U mL^{-1} penicillin/streptomycin (Nacalai Tespue, Kyoto, Japan). Adhesive adipose tissue was removed to avoid damage to the aorta, and then the aortas were washed with PBS (Nacalai Tespue). The aortas were transferred to collagenase dissolved in PBS (175 U mL^{-1}: Worthington, NJ, USA) and shaken for 30 min at 37 °C. After washing with PBS, the aortas were opened and cultured overnight at 37 °C in D-MEM. The next day, the aortas were washed with PBS and shaken with collagenase (175 U mL^{-1})/elastase (45 U mL^{-1}: Worthington) for 30 min at 37 °C to separate aortic media and adventitia. The mixture was transferred to a 50 mL tube and then 30 mL of D-MEM were added. After centrifuging at 150 g for 5 min, the supernatant was discarded, and 5 mL of D-MEM was added to the tube. Then, 1×10^6 cells mL^{-1} were seeded in T75 Flask and cultured in atmosphere of 5% CO_2/95% air at 37 °C.

RASMCs were seeded in 60-mm dishes at 5×10^5 cells/dish and cultured in complete D-MEM medium containing 10% fetal bovine serum (BIO-WEST, UT, USA) and 100 U/mL penicillin/streptomycin (Nacalai Tesque) in a humidified atmosphere of 5% CO_2/95% air at 37 °C. Cells were serum-starved for 24 h and treated with (0–300 μM) CPFX, LVFX, and MFLX for 96 h.

2.2. Western blot analysis

Proteins were isolated from RASMCs using lysis buffer (50 mM HEPES, 50 mM NaCl, 5 mM EDTA, 1% Triton X-100, 1mM Na_3VO_4, 50 mM NaF, 10 mM NAPP and 1 mM PMSF) containing 1% phosphatase and 2% protease inhibitor cocktail (Nacalai Tesque). Equal amounts of total protein (10 μg/30 μL) were subjected to sodium dodecyl sulfate (SDS) polyacrylamide gel electrophoresis (10.5%) and transferred to polyvinylidene difluoride membranes (Millipore, MA, USA), followed by incubation with Blocking One (Nacalai Tesque) for 60 min at 20–28 °C.

The primary antibodies used were rabbit anti-SM22α (1:1000 dilution; Proteintech), mouse anti-α-SMA (1:1000 dilution; Thermo Fisher Scientific, MA, USA), rabbit anti-SMMHC (1:1000 dilution; Proteintech), goat anti-caldesmon (1:1000 dilution; Santa Cruz Biotechnology, TX, USA), and rabbit anti-β-actin (1:1000 dilution; Bioss Antibodies, MA, USA). The membranes were incubated overnight at 4 °C with primary antibodies, and then incubated with secondary horseradish peroxidase-conjugated antibodies (1:10000 dilution; Bio-Rad Laboratories, CA, USA) for 60 min at 20–28 °C. Membranes were developed using an ImmunoStar® LD (Fujifilm Wako Pure Chemical Corporation, Osaka, Japan). Band images were visualized using a FluorChem SP imaging system (Alpha Innotech, CA, USA). Band intensities were quantified using the ImageJ software.

2.3. Real-time quantitative reverse transcription-polymerase reaction (qRT-PCR)

Total RNA from RASMCs was extracted using an RNeasy Mini RNA Extraction kit (Qiagen, Tokyo, Japan) according to the manufacturer's instructions. RNA was reverse

transcribed with a Superscript® VILO™ Synthesis kit (Invitrogen, Carlsbad, CA, USA) using random primers. cDNA extraction was determined by real-time qPCR using a MX3000P real-time PCR system (Agilent Technologies, Santa Clara, CA, USA) and normalized using the housekeeping gene ß-actin. PCR products were quantified using a Thunderbird™ SYBR® qPCR Mix (Toyobo, Osaka, Japan). Primers used for PCR reactions (forward and reverse, respectively) were: SM22α (5′-GAG CGG CTA GTG GAG TGG ATT G-3′ and 5′-AGG CAC CTT CAC TGG CTT GGA T-3′); α-SMA (5′-CGA TAG AAC ACG GCA TCA TCA-3′ and 5′-TTC GTA CAC GCT CTT CTC CAG GGA-3′); SMMHC (5′-GAA AGC GAT GGT CAA CAA AGA T-3′ and 5′-ACA CAG AAG AGT CCC GAG TAA G-3′); caldesmon (5′-TGG TCT CCA AGA TTG ACA GCC-3′ and 5′-ACA TGC TCT TGA TAT TGC GGA C-3′), ß-actin (5′-CCC ATC TAT GAG GGT TAC GC-3′ and 5′-TTT AAT GTC ACG CAC GAT TTC-3′). cDNAs were amplified through 50 cycles (denaturation at 95 °C for 60 s; annealing at 53 °C for 60 s; extension at 72 °C for 90 s).

2.4. Statistical analyses

Statistical analyses were performed using GraphPad Prism 9 software (GraphPad, CA, USA). Data are presented as the mean ± standard error of the mean (SEM). The statistical significance of comparisons in each graph was determined using one-way analysis of variance (ANOVA) with Tukey's multiple comparisons post hoc test. Statistical significance was set at $P < 0.05$.

3. Results

3.1. Dose- and time-dependent expression of SM22α protein

RASMCs were treated with MFLX, CPFX, and LVFX at 1, 3, 10, 30, 100, and 300 μM for 96 h. MFLX significantly decreased the expression of SM22α protein in RASMCs in a dose-dependent manner, and significantly decreased it at 100 μM and 300 μM ($p < 0.05$ and $p < 0.0001$, respectively) (Fig. 1A). In addition, CPFX and LVFX significantly decreased the expression of SM22α protein in RASMCs; the greatest decrease was observed at 300 μM ($p < 0.0001$ and $p < 0.05$, respectively) (Fig. 1B and C).

Next, RASMCs were treated with MFLX, CPFX, and LVFX (300 μM) for 0, 48, 72, and 96 h. MFLX, CPFX, and LVFX decreased the expression of SM22α protein in RASMCs in a time-dependent manner, with the most significant decrease at 96 h. MFLX significantly decreased the expression of SM22α protein in RASMCs at 72 and 96 h ($p < 0.001$ and $p < 0.0001$, respectively) (Fig. 2A). CPFX decreased the expression of SM22α protein in RASMCs in a time-dependent manner after 48 h (Fig. 2B). LVFX also significantly decreased the expression of SM22α protein in RASMCs at 72 and 96 h (both $p < 0.0001$) (Fig. 2C).

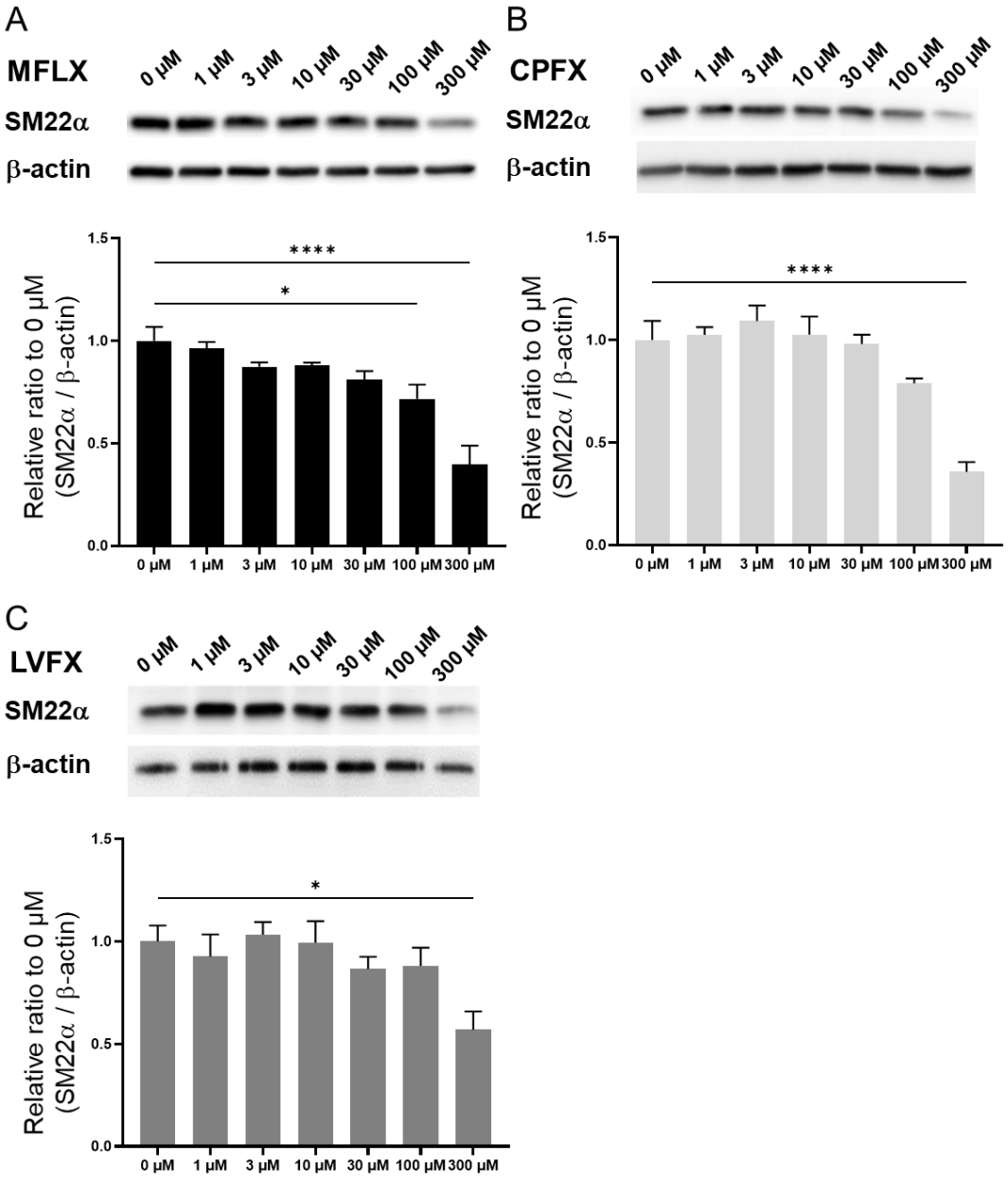

Fig. 1 Dose-dependent effects of MFLX, CPFX, and LVFX on the expression of SM22α protein in RASMCs

Representative bands of SM22α in MFLX (A) CPFX (B) and LVFX (C) treated RASMCs (upper panel). Quantitative analysis of band intensities showing expression of SM22α proteins (bottom panel). Cells were treated with MFLX, CPFX, and LVFX (10, 30 100 and 300 μM) for 96 h. Bars represent the mean ± SEM (n = 3–6).

*P < 0.05, ****P < 0.0001

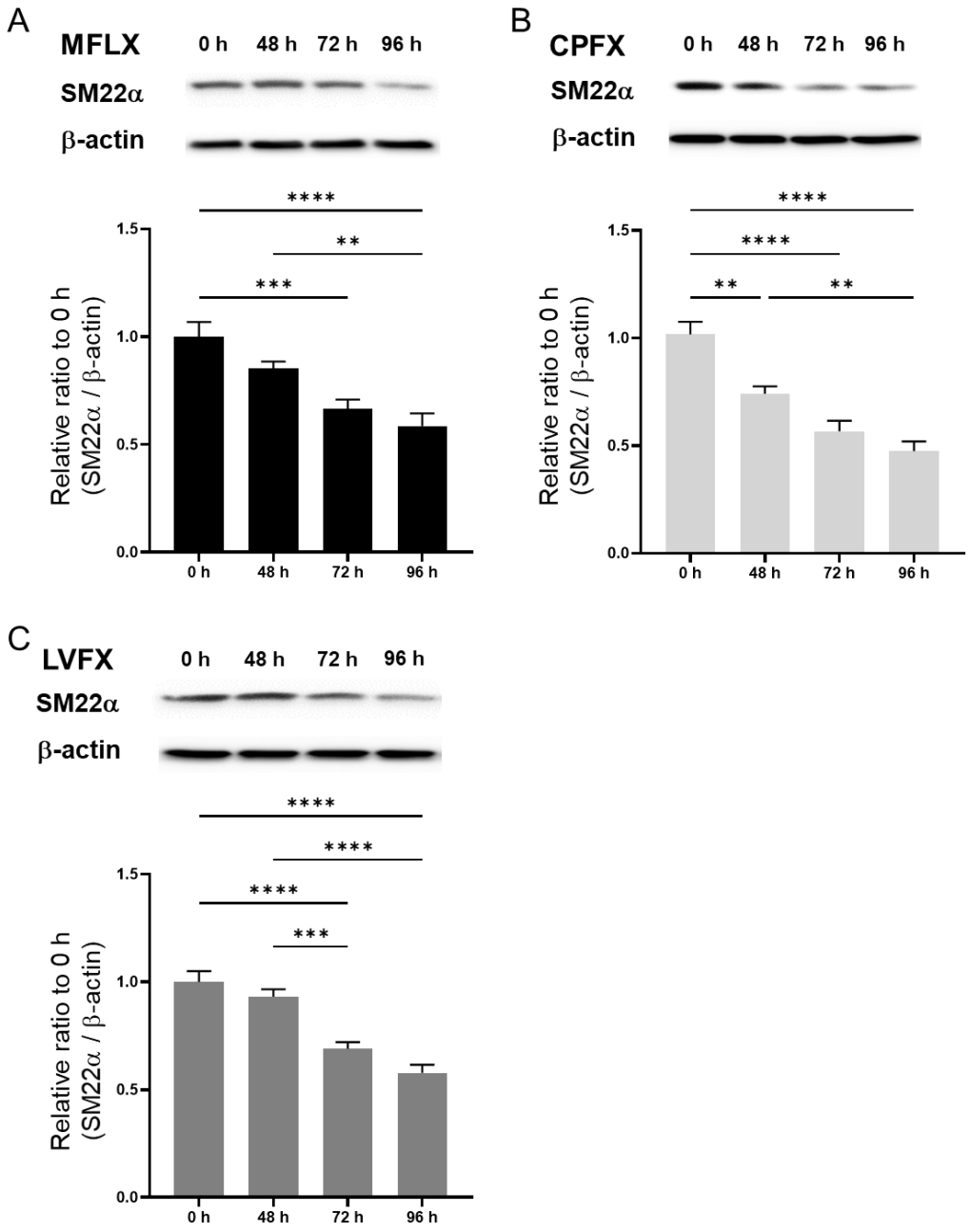

Fig. 2 Time-dependent effects of MFLX, CPFX, and LVFX on the expression of SM22α protein in RASMCs

Representative bands of SM22α in MFLX (A) CPFX (B) and LVFX (C) treated RASMCs (upper panel). Quantitative analysis of band intensities showing expression of SM22α proteins (bottom panel). Cells were treated with MFLX, CPFX, and LVFX (300 μM) for 0, 48, 72 and 96 h. Bars represent the mean ± SEM (n = 7–9).

**P < 0.01, ***P < 0.001, ****P < 0.0001.

3.2. Expression comparison of VSMCs contractile phenotype markers among fluoroquinolone antibiotics

RASMCs were treated with 300 μM fluoroquinolone antibiotics for 96 h and the expression of VSMC contractile phenotype markers was compared. CPFX and MFLX significantly decreased the expression of SM22α protein in RASMCs compared with vehicle (both $p < 0.0001$) (Fig. 3A). Furthermore, CPFX and MFLX significantly decreased the expression of SM22α protein in RASMCs compared with LVFX ($p < 0.05$ and $p < 0.01$, respectively) (Fig. 3A). CPFX and MFLX significantly decreased the expression of α-SMA protein in RASMCs compared with vehicle ($p < 0.05$ and $p < 0.01$, respectively) (Fig. 3A). All three fluoroquinolone antibiotics significantly decreased the expression of SMMHC protein in RASMCs compared with vehicle (MFLX, $p < 0.0001$; CPFX, $p < 0.05$; and LVFX, $p < 0.01$) (Fig. 3C). Moreover, all three fluoroquinolone antibiotics significantly decreased the expression of caldesmon protein compared with vehicle in RASMCs (MFLX, $p < 0.0001$; CPFX, $p < 0.05$; and LVFX, $p < 0.0001$) (Fig. 3D).

CPFX and MFLX significantly decreased the mRNA levels of SM22α, α-SMA, SMMHC, and caldesmon compared with vehicle (Fig. 4A–D). Conversely, LVFX had no effect on the mRNA expression of SM22α, α-SMA, SMMHC, and caldesmon.

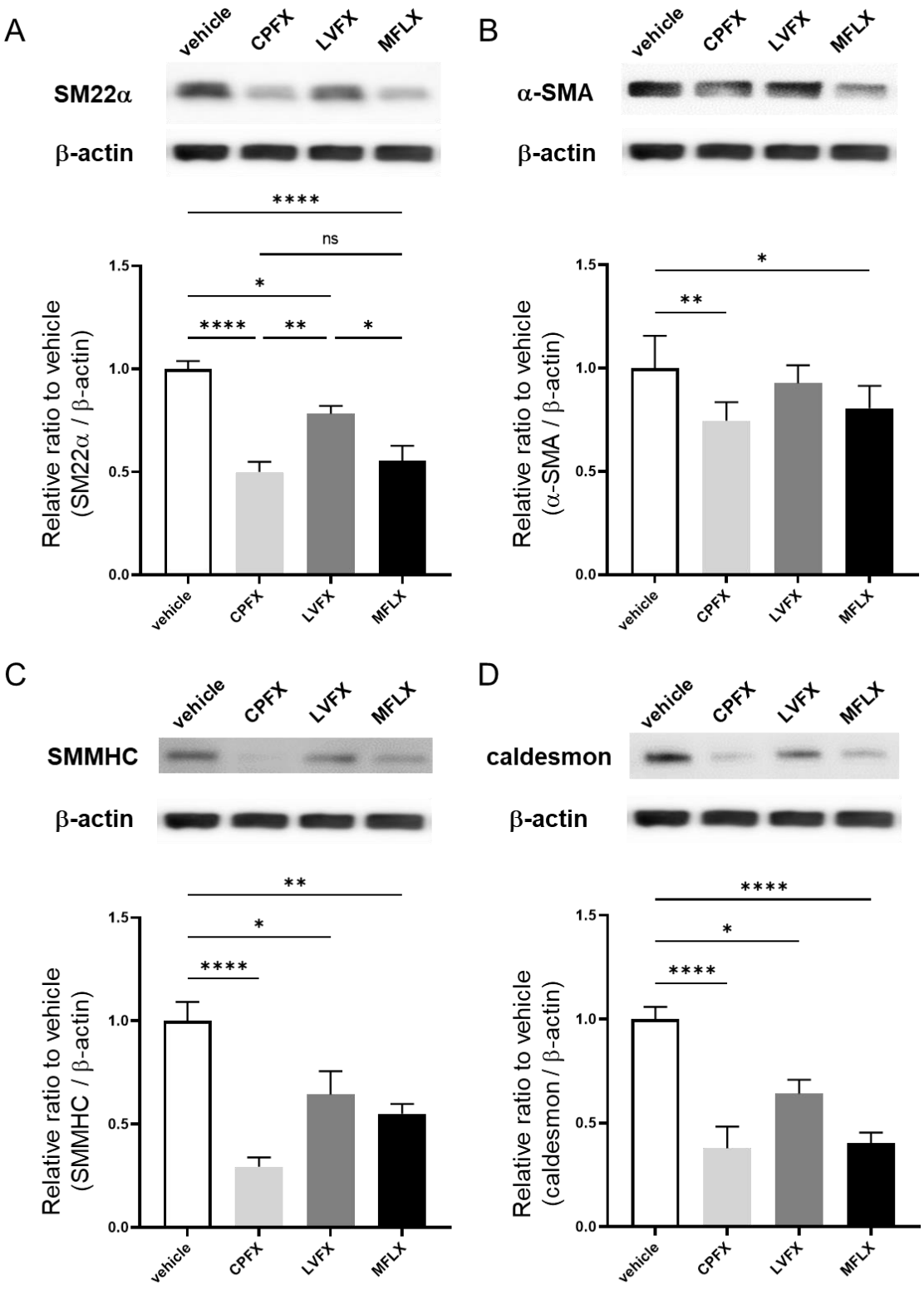
A
vehicle
CPFX
LVFX
MFLX
SM22α
β-actin
****
ns
*
****
**
*
Relative ratio to vehicle
(SM22α / β-actin)
1.5
1.0
0.5
0.0
vehicle
CPFX
LVFX
MFLX
B
vehicle
CPFX
LVFX
MFLX
α-SMA
β-actin
*
**
Relative ratio to vehicle
(α-SMA / β-actin)
1.5
1.0
0.5
0.0
vehicle
CPFX
LVFX
MFLX
C
vehicle
CPFX
LVFX
MFLX
SMMHC
β-actin
**
*
****
Relative ratio to vehicle
(SMMHC / β-actin)
1.5
1.0
0.5
0.0
vehicle
CPFX
LVFX
MFLX
D
vehicle
CPFX
LVFX
MFLX
caldesmon
β-actin
****
*
****
Relative ratio to vehicle
(caldesmon / β-actin)
1.5
1.0
0.5
0.0
vehicle
CPFX
LVFX
MFLX

Fig. 3 Effect of treatment with CPFX, LVFX, and MFLX (300 μM) for 96 h on the expression of the VSMC contractile phenotype marker proteins in RASMCs

Representative bands of SM22α (A), α-SMA (B), SMMHC (C) and caldesmon (D) in CPFX-, LVFX-, and MFLX-treated RASMCs (upper panel). Quantitative analysis of band intensities showing expression of SM22α (A), α-SMA (B), SMMHC (C) and caldesmon (D) proteins (bottom panel). Cells were treated with CPFX, LVFX, and MFLX (300 μM) for 96 h. Bars represent the mean ± SEM (n = 7–9). *P < 0.05, **P < 0.01, ****P < 0.0001.

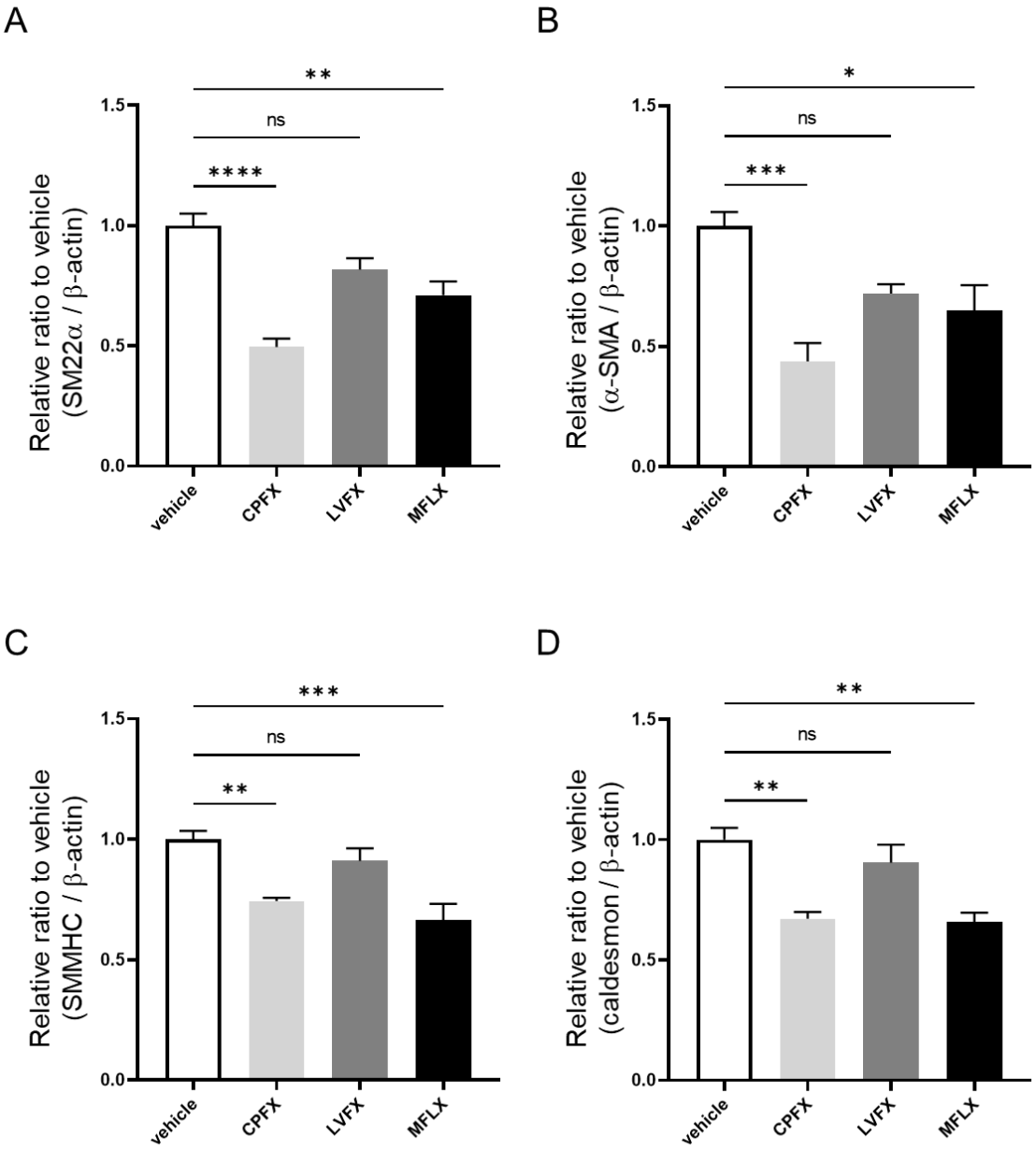
A
B
C
D
Relative ratio to vehicle
(SM22α / β-actin)
(α-SMA / β-actin)
(SMMHC / β-actin)
(caldesmon / β-actin)
1.5
1.0
0.5
0.0
ns
**
****
***
*
vehicle
CPFX
LVFX
MFLX

Fig. 4 Effect of treatment with CPFX, LVFX, and MFLX (300 μM) for 96 h on the mRNA expression of the VSMC contractile phenotype marker proteins in RASMCs.
Bar graphs showing the mRNA expression of SM22α (A), α-SMA (B), SMMHC (C) and caldesmon (D), based on quantitative real-time RT-PCR analyses. Cells were treated with CPFX, LVFX, and MFLX (300 μM) for 96 h. Results are expressed as relative ratio to vehicle cells. ß-actin was used as loading control. Bars represent the mean ± SEM (n = 5). *P < 0.05, **P < 0.01, ***P < 0.001 and ****P < 0.0001.

4. Discussion

In this chapter, we compared the effects of three fluoroquinolone antibiotics, MFLX, CPFX, and LVFX, on the expression of the VSMC contractile phenotype markers in RASMCs.

The expression levels of SM22α mRNA and protein were lower in the aortic wall of AAA model animals than in controls [10]. In this study, MFLX, CPFX, and LVFX significantly decreased the expression of SM22α in RASMCs in a dose- and time-dependent manner; the greatest decrease was observed at 300 μM for 96 h (Fig. 1 and 2). Therefore, MFLX, CPFX, and LVFX may contribute to the onset and exacerbation of AAD by inducing weakening of the aortic media owing to the loss of the RASMCs.

Phenotype switching from contractile to synthetic in VSMCs induces AAD [11, 12]. Since all three drugs, MFLX, CPFX, and LVFX, significantly decreased SM22α, we also focused on other markers of the VSMC contractile phenotype and compared their expression among the three drugs. We found that CPFX and MFLX significantly decreased the expression of SM22α, α-SMA, SMMHC, and caldesmon proteins in RASMCs compared with vehicle (Fig. 3). On the other hand, LVFX significantly decreased the expression of SM22α, SMMHC, and caldesmon proteins in RASMCs compared with vehicle, but did not significantly decrease the expression ofα-SMA protein (Fig. 3). Furthermore, MFLX and CPFX significantly decreased the expression of SM22α, α-SMA, SMMHC, and caldesmon in mRNA levels in RASMCs compared with vehicle, but LVFX did not significantly decrease these (Fig. 4). The three drugs, MFLX, CPFX, and LVFX decreased the expression of the VSMC contractile phenotype markers,

suggesting that fluoroquinolone antibiotics may increase the risk of onset and exacerbation AAD. LVFX may have a lower risk compared to that of CPFX and MFLX. In the present study, MFLX, CPFX, and LVFX may induce the onset and exacerbation of AAD through weakening of the aortic media through VSMC loss and phenotype switching from contractile to synthetic. Among the three drugs, MFLX and CPFX presented a higher risk for the development and exacerbation of AAD than LVFX. Therefore, in patients with AAD and patients with a high risk of developing AAD, LVFX should be selected with preference to MFLX and CPFX if using fluoroquinolone antibiotics.

References

[1] A.C. Bennett, C.L. Bennett, B.J. Witherspoon, K.B. Knopf, An evaluation of reports of ciprofloxacin, levofloxacin, and moxifloxacin-association neuropsychiatric toxicities, long-term disability, and aortic aneurysms/dissections disseminated by the Food and Drug Administration and the European Medicines Agency, Expert Opin Drug Saf 18 (2019) 1055-1063.

[2] P. Rawla, M.L. El Helou, A.R. Vellipuram, fluoroquinolones and the risk of aortic aneurysm or aortic dissection: A systematic review and meta-analysis, Cardiovasc Hematol Agents Med Chem 17 (2019) 3-10.

[3] S. Singh, A. Nautiyal, Aortic Dissection and aortic aneurysms associated with fluoroquinolones: A systematic review and meta-analysis, Am J Med 130 (2017) 1449-1457.e1449.

[4] E.L. Chaikof, R.L. Dalman, M.K. Eskandari, B.M. Jackson, W.A. Lee, M.A. Mansour, T.M. Mastracci, M. Mell, M.H. Murad, L.L. Nguyen, G.S. Oderich, M.S. Patel, M.L. Schermerhorn, B.W. Starnes, The Society for Vascular Surgery practice guidelines on the care of patients with an abdominal aortic aneurysm, J Vasc Surg 67 (2018) 2-77.e72.

[5] P.E. Norman, J.A. Curci, Understanding the effects of tobacco smoke on the pathogenesis of aortic aneurysm, Arterioscler Thromb Vasc Biol 33 (2013) 1473-1477.

[6] K.C. Kent, Clinical practice. Abdominal aortic aneurysms, N Engl J Med 371 (2014) 2101-2108.

[7] V.B. Kokje, J.F. Hamming, J.H. Lindeman, Editor's Choice - Pharmaceutical management of small abdominal aortic aneurysms: A systematic review of the clinical evidence, Eur J Vasc Endovasc Surg 50 (2015) 702-713.

[8] S.S. Rensen, P.A. Doevendans, G.J. van Eys, Regulation and characteristics of vascular smooth muscle cell phenotypic diversity, Neth Heart J 15 (2007) 100-108.

[9] S. Allahverdian, C. Chaabane, K. Boukais, G.A. Francis, M.L. Bochaton-Piallat, Smooth muscle cell fate and plasticity in atherosclerosis, Cardiovasc Res 114 (2018) 540-550.

[10] G. Ailawadi, C.W. Moehle, H. Pei, S.P. Walton, Z. Yang, I.L. Kron, C.L. Lau, G.K. Owens, Smooth muscle phenotypic modulation is an early event in aortic aneurysms, J Thorac Cardiovasc Surg 138 (2009) 1392-1399.

[11] N. Mao, T. Gu, E. Shi, G. Zhang, L. Yu, C. Wang, Phenotypic switching of vascular smooth muscle cells in animal model of rat thoracic aortic aneurysm, Interact Cardiovasc Thorac Surg 21 (2015) 62-70.

[12] Y. Shao, G. Li, S. Huang, Z. Li, B. Qiao, D. Chen, Y. Li, H. Liu, J. Du, P. Li, Effects of extracellular matrix softening on vascular smooth muscle cell dysfunction, Cardiovasc Toxicol 20 (2020) 548-556.

General discussion

Considering the usefulness and frequency of use of fluoroquinolone antibiotics in a wide range of infectious diseases, it is urgent to establish measures to prevent, reduce, and avoid AAD induced by fluoroquinolone antibiotics.

In this study, it is suggested that fluoroquinolone antibiotics may induce the development and exacerbation of AAD. In addition, MFLX and CPFX may be associated with a higher risk of ADD onset and exacerbation than LVFX, based on the risk comparison among the three drugs. Based on these findings, the potentially elevated risk of fluoroquinolone antibiotics on the development and exacerbation of AAD at the start or during drug treatment needs to be considered. Furthermore, selection of the suitable antibiotic for fluoroquinolone antibiotic drug therapy is important in patients at high risk for AAD.

In future, we may be able to predict, reduce, and avoid adverse effects of fluoroquinolone antibiotics, which will significantly improve the safety and efficacy of these drugs.

Published and submitted papers

1. **Inada K**, Koga M, Yamada A, Dohgu S, Yamauchi A. Moxifloxacin induces aortic aneurysm and dissection by increasing osteopontin in mice. *Biochem Biophs Res Commun* 2022; 12; 629: 1-5.

2. Koga M, Kanaoka Y, **Inada K**, Omine S, Kataoka Y, Yamauchi A. Hesperidin blocks varenicline-aggravated atherosclerotic plaque formation in apolipoprotein E Knockout mice by downregulating net uptake of oxidized low-density lipoprotein in macrophages. J Pharmacol Sci 2020; 143(2): 106-11.

3. Koga M, Kanaoka Y, Okamoto M, Nakao Y, **Inada K**, Takayama S, Kataoka Y, Yamauchi A. Varenicline aggravates atherosclerotic plaque formation in nicotine-pretreated ApoE knockout mice due to enhanced oxLDL uptake by macrophages through downregulation of ABCA1 and ABCG1 expression. J Pharmacol Sci 2020; 142(1): 9-15.

Acknowledgments

I would like to express my sincere appreciation to Prof. Dr. Atsushi Yamauchi, Department of Pharmaceutical Care and Health Sciences, Faculty of Pharmaceutical Sciences, Fukuoka University, for his endless help and encouragement.

I would like to express my gratitude to Associate Prof. Dr. Mitsuhisa Koga, Department of Drug Design and Drug Delivery, Faculty of Pharmaceutical Sciences, Fukuoka University, for their helpful suggestion and endless help.

I would like to express my gratitude to Prof. Dr. Shinya Dohgu, Department of Pharmaceutical Care and Health Sciences, Faculty of Pharmaceutical Sciences, Fukuoka University, and Associate Prof. Dr. Mitsuhisa Koga, Department of Drug Design and Drug Delivery Faculty of Pharmaceutical Sciences, Fukuoka University, for their useful advice and discussion.

I would like to thank Associate Prof. Dr. Fuyuko Takata, Associate Prof. Dr. Shinsuke Nakagawa, Assistant Prof. Dr. Junichi Matsumoto, Assistant Prof. Dr. Takuro Iwao, Department of Pharmaceutical Care and Health Sciences, Faculty of Pharmaceutical Sciences, Fukuoka University, for their advice and help.

I would like to thank the faculty of Department of Pharmaceutical Care and Health Sciences, Faculty of Pharmaceutical Sciences, Fukuoka University for their support.

Finally, I would like to express thanks to my family for their encouragement and loving support.